To be submitted to
Nuclear Instr. & Meth.

ISTITUTO NAZIONALE DI FISICA NUCLEARE
Laboratori Nazionali di Frascati

LNF-80/9(P)
26 Febbraio 1980

G.P. Capitani, E. De Sanctis, P. Di Giacomo, C. Guaraldo, S. Gentile, V. Lucherini, E. Polli, A.R. Reolon and R. Scrimaglio: A PAIR SPECTROMETER FOR THE LEALE MONOCHROMATIC PHOTON BEAM OF FRASCATI LABORATORIES.

Servizio Documentazione
dei Laboratori Nazionali di Frascati
Cas. Postale 13 - Frascati (Roma)

INFN - Laboratori Nazionali di Frascati
Servizio Documentazione

LNF-80/9(P)
26 Febbraio 1980

G.P. Capitani, E. De Sanctis, P. Di Giacomo, C. Guaraldo, S. Gentile, V. Lucherini, E. Polli, A.R. Reolon and R. Scrimaglio: A PAIR SPECTROMETER FOR THE LEALE MONOCHROMATIC PHOTON BEAM OF FRASCATI LABORATORIES.

1. - INTRODUCTION.

The determination of photonuclear cross sections requires the knowledge of the primary photon spectrum. The intensity and the energy spectrum of the Frascati positron annihilation photon beam[1] are measured by a Komar et al. type quantameter[2] and a pair spectrometer.

The present paper concerns the study and the design of the pair spectrometer. In section 2. the general layout of the facility is reported. In section 3. the main characteristics of the magnet are given. Section 4. is concerned with the optical properties of the spectrometer. The detection system, with the associated electronics, is described in section 5. In Section 6. the calculation of the spectrometer response function is reported. In section 7. the experimental photon energy spectrum, at positron energy $E_+ = 200$ MeV, compared with the calculated one, is given.

2. - GENERAL LAYOUT OF THE FACILITY.

The experimental set up of the photon beam facility is shown in Fig. 1. Positrons leave the beam pipe through an aluminium window 0.06 mm thick, annihilate on a liquid hydrogen target 0.011 radiation lenghts thick, and are deflected down on a Farady cup by a dumping magnet. The photon beam is defined by four circular lead collimators (10.5 mm, 11.0 mm, 12.5 mm and 13.8 mm diameters; 16.7 cm, 16.7 cm, 10.3 cm and 12.0 cm lenghts, respectively) inserted in the yoke of the dumping magnet and in the gap of the sweeping magnet B_7 of Fig. 1. As a spectrometer, an old rectangular flat pole (40x90 cm^2 size, 15 cm gap) C-type magnet, which had seen prior service at the Frascati synchrotron, has been used. Photons enter through a hole, 4 cm diameter, opened in the yoke of the magnet and hit the conversion target. In order to reduce background production from air, the beam line from the hydrogen target to the spectrometer is under vacuum.

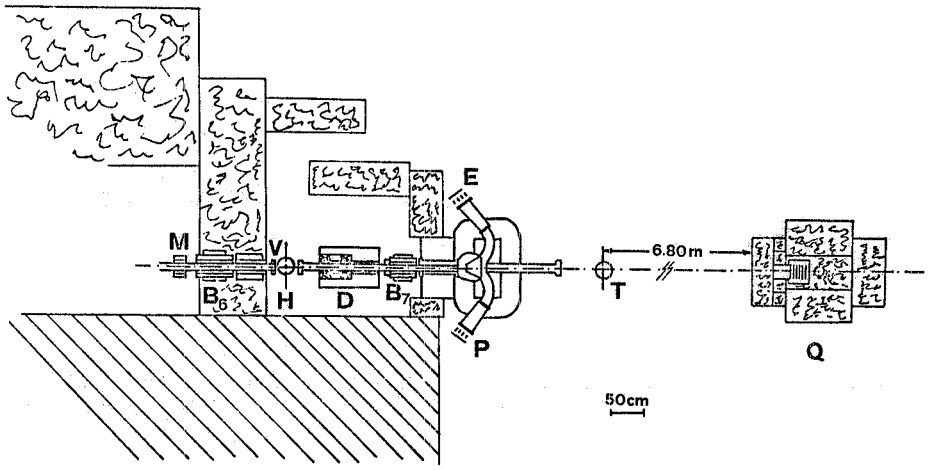

FIG. 1 - Photon beam layout: M positron ferrite-induction monitor; B_6 steering magnet; V aluminium window (0.06 mm thick); H liquid hydrogen target (0.011 radiation lenghts thick); D dumping magnet, B_7 sweeping magnet; PS pair spectrometer; E, P electron and positron detectors; T photoreaction target; Q quantameter.

3. - THE MAGNET.

To achieve the best conditions in utilizing the magnet as a pair spectrometer, a careful study of its optical properties has been devoted. The values of the magnetic field have been measured on three horizontal planes, the median one and two planes at + 2.5 cm and + 5.0 cm[3].

In each plane the main field component B_z has been measured on a variable mesh (2 cm or 1 cm according to the field gradient value), utilizing a F.W. Bell 8860 model gaussmeter with a Hall probe 2x2 mm^2 sensitivity area.

The gaussmeter has been calibrated versus a nuclear magnetic resonance fluxmeter with 0.1% precision.

The measurements of the energy spectrum at photon energies up to 300 MeV requires the maximum field value of 13.8 kG. Therefore, due to the non linearity of the excitation curve (see Fig. 2), four field maps have been measured at B=9.0 kG, 10.5 kG, 12.0 kG and 13.8 kG for each of the above mentioned planes. Moreover, in order to check the symmetry of the field respect to the median plane, measurements on the planes at - 2.5 cm

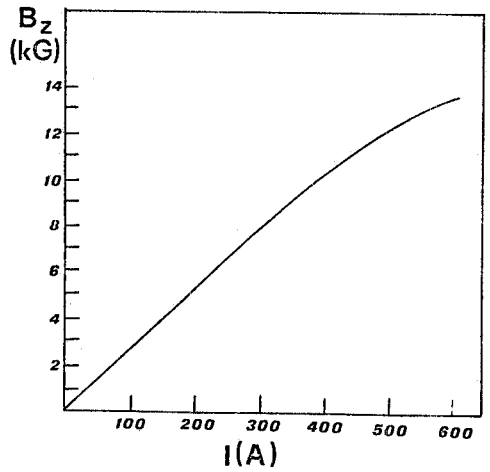

FIG. 2 - Magnet excitation curve.

and - 5.0 cm have been also performed. The results have shown a fairly good symmetry.

A second Hall probe, inserted at the center of the pole face, allowed to check continuously the central field value.

The total relative error in measuring the magnetic field is about 0.5%. In order to perform a numerical integration of the equation of motion, field maps at a constant mesh (1 cm) have been derived by interpolating the measured values with the "four - points Lagrange method". In Fig. 3 the isofield curves, obtained for the 13.8 kG value, are given.

As a consequence of a slight misalignment of the poles, the components of the magnetic field on the median plane (B_x and B_y) are not equal to zero, but always less than 0.5% of B_z and therefore are negligible.

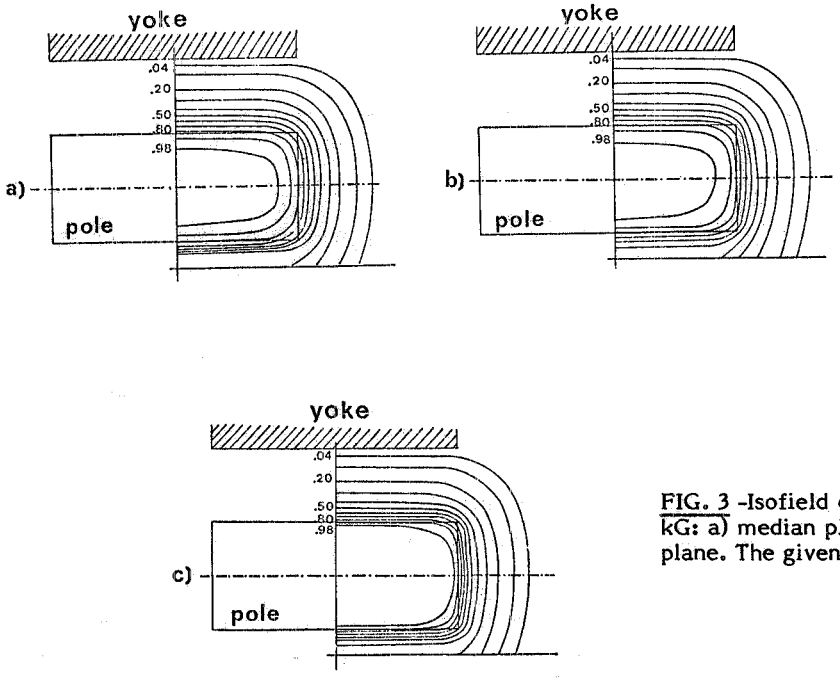

FIG. 3 -Isofield curves for a centre field B=13.8 kG: a) median plane; b) +2.5 cm plane, c) +5 cm plane. The given values are percent of B.

4. - OPTICAL PROPERTIES OF THE SPECTROMETER.

The optical properties of the spectrometer have been studied by evaluating numerically over a thousand trajectories for each of the four center field values chosen for the maps. Each trajectory is characterized by the momentum p, the origin point in the converter and the emission angles ϑ and φ (see Fig. 4). The coordinate system used is defined in Fig. 4: the xy plane is the horizontal symmetry plane of the magnet.

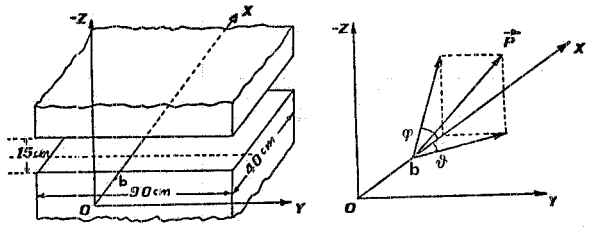

FIG. 4- Definition of coordinate system: xy is the horizontal symmetry plane of the magnet; b is the conversion target point (coordinate x=15 cm, y=z=0) p, ϑ and φ are the momentum and the angles of the electron.

For each momentum value p the trajectory which leaves the centre of the converter with $\vartheta = \varphi = 0°$ has been assumed as the central one. The magnetic field components at any points of the space have been calculated by the aid of the circuitation theorem[3]. The equation of motion has been integrated using the Hamming's method, which permits to check the error step by step and therefore to deduce the increment of the integration variable, if necessary[4].

For each field setting the best focal line has been evaluated by taking into account only trajectories starting from the center of the converter with arbitrary, but less than $|\pm 0.5°|$, ϑ and φ angles[5]. In fact, the mean emission angle of electron-positron pairs is of the order of m/E (mass and energy of the particle), which means, in our case, values always less than $|\pm 0.5°|$.

The best focal line valid for the four field configurations has the following expression:

$$y = 0.637\ x + 103.$$

The momentum values along this line have been deduced through the relation:

$$p = a + b\zeta + c\,\zeta^2 + d\,\zeta^3,$$

where ζ is the coordinate along the focal line with origin in the intersection of the focal line with the y-axis. The parameters a, b, c and d, deduced by fitting the ζ values, resulting from a ray-tracing calculations of several trajectories, are reported in Table I. The error introduced because of this procedure is always less than 0.04%. In the table the centre field and the corresponding momentum acceptance interval are also given. It results that with the above four field configurations the photon spectrum can be measured in the range (170÷300) MeV. For lower photon energies the field maps can be evaluated starting from those found at 9 kG, due to the linearity of the excitation curve.

The focalizing properties of the magnet are momentum dependent; for each field value the higher the momenta the worse they are. However, the overall error in momentum determination is always less than 0.1%.

The displacements $\Delta\zeta$ from the central trajectory due to the finite transverse dimension of the photon beam (circular shaped, $\leq$ 2 cm diameter) on the conversion target have been found as great as $\sim$3 cm (see Table II). The error magnitude is about the same for the electrons and positrons, but signs are different. As a consequence, the error Δp^- and Δp^+ on electron and positron momenta, due to the transverse dimension of the beam, are about equal in magnitude, with opposite signs. Therefore, the photon energy is effected by an error $(|\Delta p^-| - |\Delta p^+|)$ which results always less than 0.15%.

TABLE I

Values of the parameter a,b,c,d for the four centre fields B.
Δp is the spectrometer momentum acceptance.

B kG	Δp (MeV/c)	a (MeV/c)	b $\frac{MeV}{c}$ /cm	c $\frac{MeV}{c}$ /cm^2	d $\frac{MeV}{c}$ /cm^3
13.8	128÷150	125.65	0.645	$0.528\ 10^{-2}$	$-0.440\ 10^{-4}$
12.0	111÷132	110.49	0.566	$0.498\ 10^{-2}$	$-0.440\ 10^{-4}$
10.4	97÷115	96.20	0.489	$0.467\ 10^{-2}$	$-0.440\ 10^{-4}$
9.0	83÷99	82.76	0.435	$0.410\ 10^{-2}$	$-0.432\ 10^{-4}$

TABLE II

Ray tracing results for B=13.8 kG. ρ is the trajectory radius: the reported values correspond to the minimum, the central and the maximum accepted radii: y and z are the coordinates of the pair production point. ϑ and φ are the initial electron (positron) angles. $\Delta\zeta$ is the displacements from the central trajectory on the focal line.

radius	initial conditions				
(cm)	y (cm)	z (cm)	ϑ (°)	φ (°)	$\Delta\zeta$ (cm)
32	-1.0	0.0	0.5	0.0	-3.28
32	1.0	0.0	0.5	0.0	3.16
32	-1.0	0.0	-0.5	0.0	-3.27
32	1.0	0.0	-0.5	0.0	3.22
32	-1.0	0.0	0.0	±0.5	-3.25
32	1.0	0.0	0.0	±0.5	3.20
32	-1.0	0.0	0.5	±0.5	-3.29
32	-0.7	0.7	0.5	±0.5	-2.32
32	0.0	1.0	0.5	±0.5	-0.09
32	0.7	0.7	0.5	±0.5	2.20
32	1.0	0.0	0.5	±0.5	3.14
32	-1.0	0.0	-0.5	±0.5	-3.28
32	-0.7	0.7	-0.5	±0.5	-2.33
32	0.0	1.0	-0.5	±0.5	-0.08
32	0.7	0.7	-0.5	±0.5	2.21
32	1.0	0.0	-0.5	±0.5	3.21
34	-1.0	0.0	0.5	0.0	-3.13
34	1.0	0.0	0.5	0.0	2.84
34	-1.0	0.0	-0.5	0.0	-2.87
34	1.0	0.0	-0.5	0.0	3.14
34	-1.0	0.0	0.0	±0.5	-3.01
34	1.0	0.0	0.0	±0.5	2.93
34	-1.0	0.0	0.5	±0.5	-3.14
34	-0.7	0.7	0.5	±0.5	-2.25
34	0.0	1.0	0.5	±0.5	-0.18
34	0.7	0.7	0.5	±0.5	1.92
34	1.0	0.0	0.5	±0.5	2.98
34	-1.0	0.0	-0.5	±0.5	-2.89
34	-0.7	0.7	-0.5	±0.5	-2.00
34	0.0	1.0	-0.5	±0.5	0.15
34	0.7	0.7	-0.5	±0.5	2.20
34	1.0	0.0	-0.5	±0.5	3.12
36	-1.0	0.0	0.5	0.0	-3.03
36	1.0	0.0	0.5	0.0	2.55
36	-1.0	0.0	-0.5	0.0	-2.55
36	1.0	0.0	-0.5	0.0	2.94
36	-1.0	0.0	0.0	±0.5	-2.79
36	1.0	0.0	0.0	±0.5	2.74
36	-1.0	0.0	0.5	±0.5	-3.04
36	-0.7	0.7	0.5	±0.5	-2.19
36	0.0	1.0	0.5	±0.5	-0.25
36	0.7	0.7	0.5	±0.5	1.71
36	1.0	0.0	0.5	±0.5	2.55
36	-1.0	0.0	-0.5	±0.5	-2.56
36	-0.7	0.7	-0.5	±0.5	-1.76
36	0.0	1.0	-0.5	±0.5	0.21
36	0.7	0.7	-0.5	±0.5	2.13
36	1.0	0.0	-0.5	±0.5	2.95

5. - EXPERIMENTAL SET-UP.

The spectrometer vacuum chamber is made of stainless steel and consists of a cylinder (42 cm diameter) with two curved arms (see Fig. 5a). This chamber is introduced into the space between the poles when the upper pole is lifted. A vacuum of 10^{-3} mm Hg is mainteined with the help of a conventional rotary pump. Applied at the cylinder are at the entrance a tube, 12 cm diameter and 60 cm long, passing through a hole in the yoke of the magnet, and at the exit, a tube 8.3 cm diameter and 64 cm long, with a mylar window foil, 0.123 mm thick ($\sim 4.3\ 10^{-4}$ radiation lenghts).

The electron-positron pairs are produced on aluminium conversion targets applied to plexiglass rings whose a diameters are 6 cm. The rings are mounted on a turntable (see Fig. 5b) which can be positioned remotely, so that they may be interposed in the path of the beam.

We use five aluminium converters, whose tihcknesses have been chosen in order to minimize both photon beam attenuation and loss of efficiency due to particle multiple scattering and energy losses. In Table III materials, shapes and dimensions of the targets are given.

TABLE III - Conversion target characteristics.

Target n°	Material	Shape	Dimension	Thickness (mm)
1	Vacuum			
2	aluminium	rect.	3 x 6 cm^2	5 x 10^{-3}
3	aluminium	circular	Φ = 6 cm	5 x 10^{-3}
4	aluminium	circular	Φ = 6 cm	10^{-2}
5	aluminium	circular	Φ = 6 cm	3 x 10^{-2}
6	aluminium	circular	Φ = 6 cm	10^{-1}

A Hall probe, permanently inserted in a fixed position between the poles, enables a continuous check of the field value, with $\pm$ 0.5% accuracy. The magnet current is stable to 1 part in 10^4.

Electrons and positrons are deflected about 110° by the magnet, then leave the vacuum chamber, through two aluminium windows, 1 mm thick. Two identical systems of plastic scintillators are used for particle detection[6]. Each system consists of an array of four counters set along the focal line ($E_{1...4}$ and $P_{1...4}$ (dimension: 1x2x10 cm^3), 5 cm spaced), follwed by a fifth counter (E_5, P_5(dimension: 20x1x20 cm^3)). Each scintillator is coupled with a 56 AVP photomultiplier.

Both counter arrays E_i, P_i are mounted on a frame which can be shifted along the focal line, so that it is possible, with successive setting, to explore the whole line and to measure the relative detection efficiency of the counters, by putting each of them in the position of its neighbours. For each field configuration the spectrometer defines seven independent energy channels.

In Fig. 6 the electronic block diagram is given: the $E_i(P_i)$ discriminator outputs are sent to an OR circuit and then to a double coincidence with the $E_5(P_5)$ counter. Real and accidental coincidence signals enable the acquisition via CAMAC on a PDP 15/30 computer of the signals from the E_i and P_i counters.

The photon energy spectrum is displayed on-line on a storage display scope.

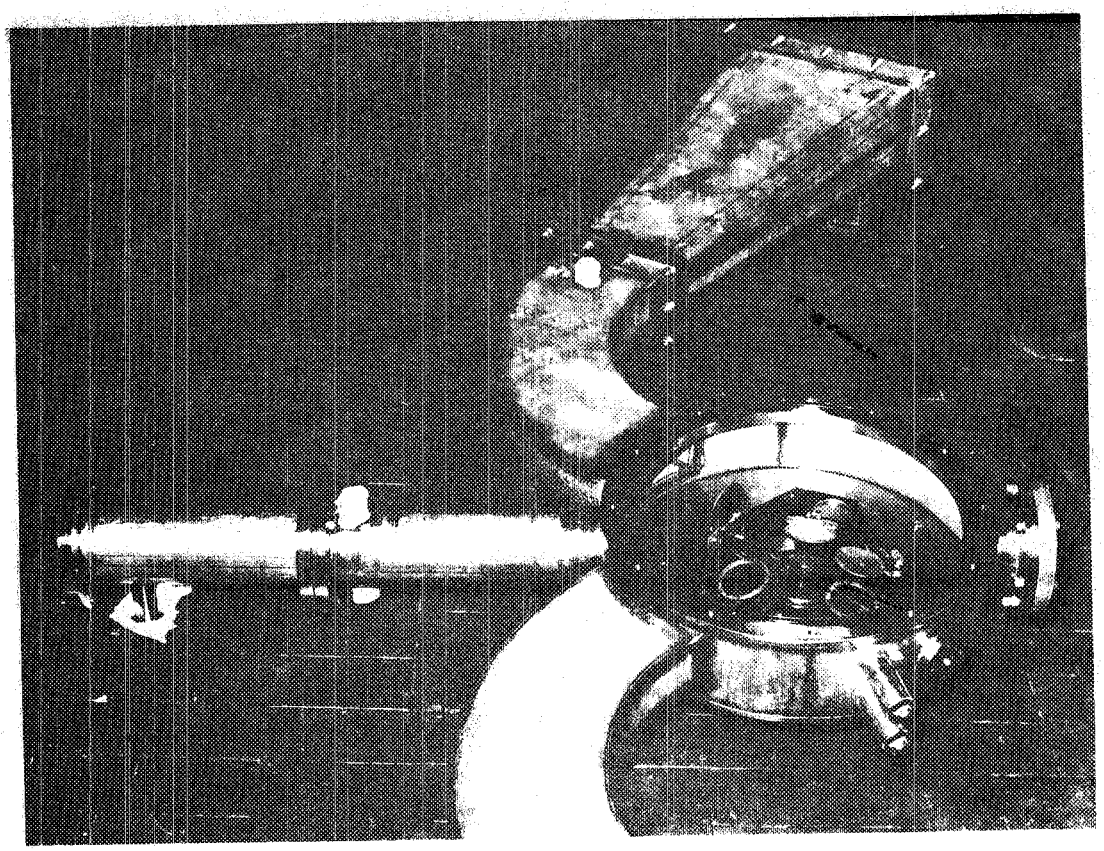

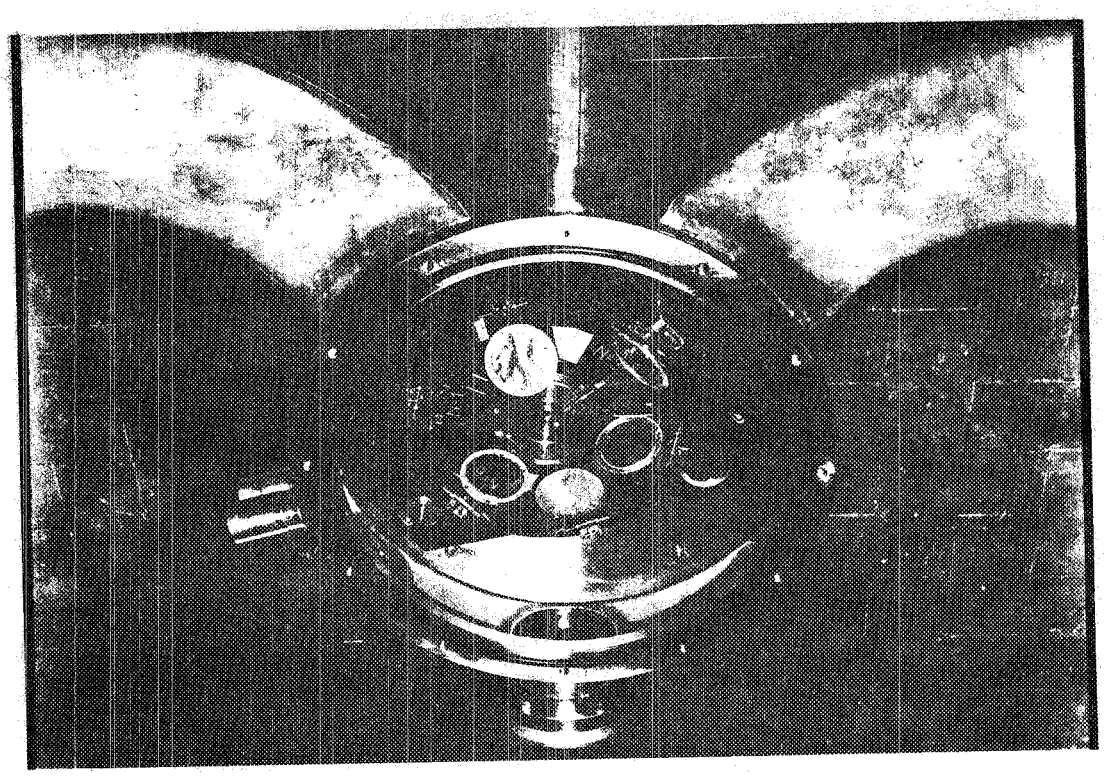

FIG. 5 - a) spectrometer vacuum chamber, b) target holder system.

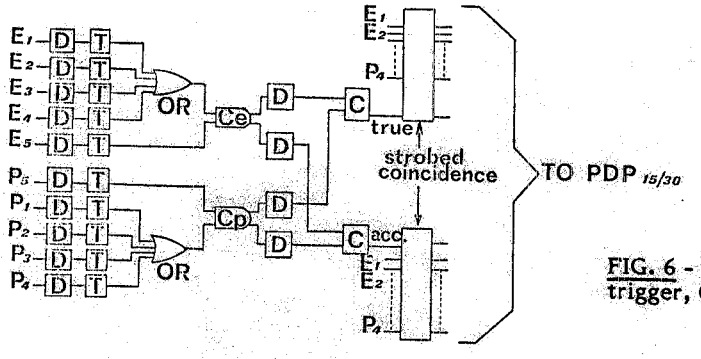

FIG. 6 - Electronic block diagram (D delay, T trigger, C coincidence).

6. - CALCULATION OF THE RESPONSE FUNCTION.

The counting rate $N_{il}(B)$ can be deduced from the photon flux $\Phi(k)$, impinging on the conversion target, and from the response function $A_{il}(k,B)$ through the following relation:

$$N_{il}(B) = \int_0^\infty \Phi(k) A_{il}(k,B) dk \qquad (i,l=1...4)$$

where k is the photon energy, B the magnetic field and (i,l) specifies the involved counter couple.

For $\Phi(k) = \Phi_o = \text{const.}$, the efficiency η_{il}, defined as the probability of pair production and detection, is given by:

$$\eta_{il}(B) = \frac{N_{il}(B)}{\Phi_o} = \int_0^\infty A_{il}(k,B)\, dk.$$

In order to calculate $A_{il}(k,B)$ the following assumptions have been made:

- photon beam emittance on the conversion target deduced by a Monte Carlo calculation of the positron annihilation and bremsstrahlung processes through the hydrogen target[7];
- validity of the Davis-Bethe-Maximon[8] formula for the elastic scattering part and of the Wheeler-Lamb[8] formula for the inelastic part of the pair production process on a screened point nucleus, for extreme relativistic energies, as summmarized by Tsai[9];
- multiple scattering of the electron-positron pairs in the aluminium converter foil negligeable;
- energy losses due to collisions and by radiation negligeable;
- ζ coordinate along the focal line evaluated through an approximate function of trajectory variables. This function has been deduced from a best fit of the ζ values, obtained from an exact ray-tracing calculation of thousand trajectories[10];
- 100% detection efficiency of plastic counters.

With these assumptions and extensive use of Monte Carlo tecnique the results of Figs. 7 and 8 have been obtained. In Fig. 7 the response functions $A_{il}(k,B)$ for the sixsteen counter couples (corresponding to seven independent energy channels) at a magnetic field B=9 kG are shown. In Fig. 8 the response function $A_{23}(k,B)$, relative to the counter couple (2,3), at five different field B values is given.

The resolution, defined as the relative FWHM of the response function, is plotted in Fig. 9 as a function of the central energy value k_o, for the counter couple (2,3). Similar plots for the other counter couples have been found.

At last, in Fig. 10, the efficiency $\eta_{23}(k_o)$ of the couple E_2P_3 is plotted as a function of k_o.

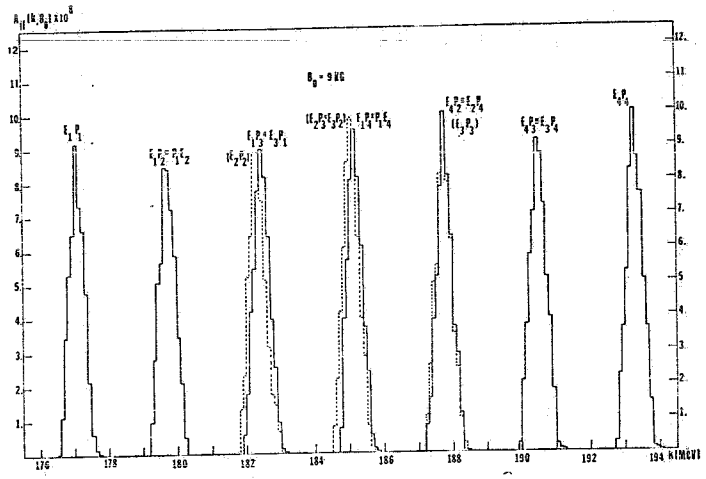

FIG. 7- Response functions $A_{ij}(k, B_o)$ for the sixteen counter couples E_iP_j at a magnetic field B_o=9 kG. (Dashed lines refer to the couples in brackets). Conversion target: aluminium foil 5 x 10^{-3} radiation lenghts thick; beam area circular, Φ= 2.0 cm.

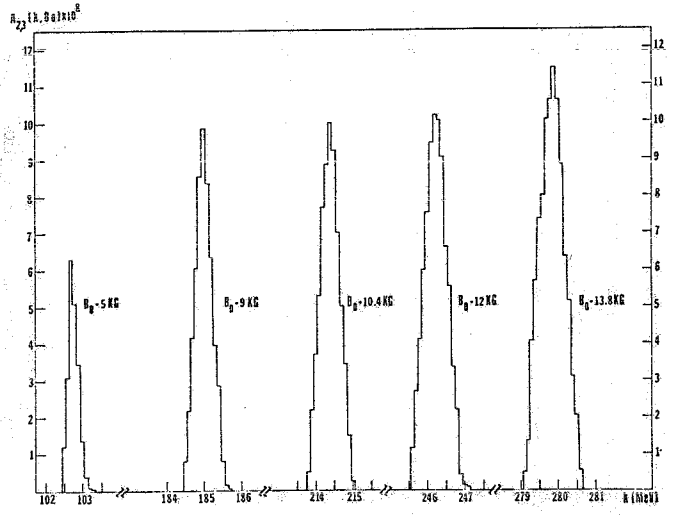

FIG. 8 - Response function A_{23} (k, B_o) for E_2P_3 counter couple at five different field B_o values. Same parameters as Fig. 7.

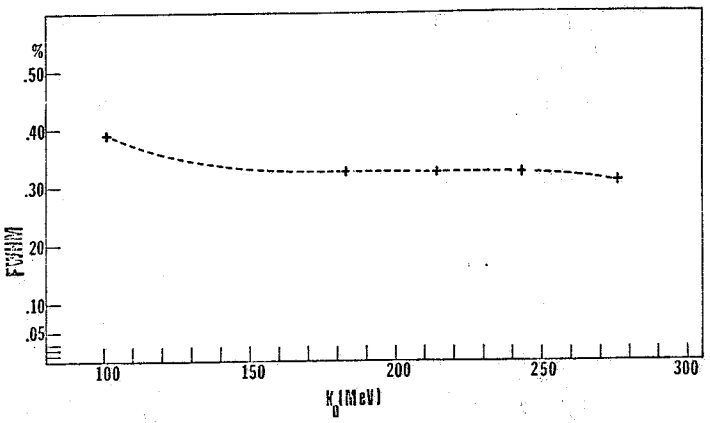

FIG. 9- Relative FWHM of $A_{23}(k,B)$ as a function of k_o. k_o is the central photon energy measured by E_2P_3 couple for different B values. Same parameters as Fig. 7.

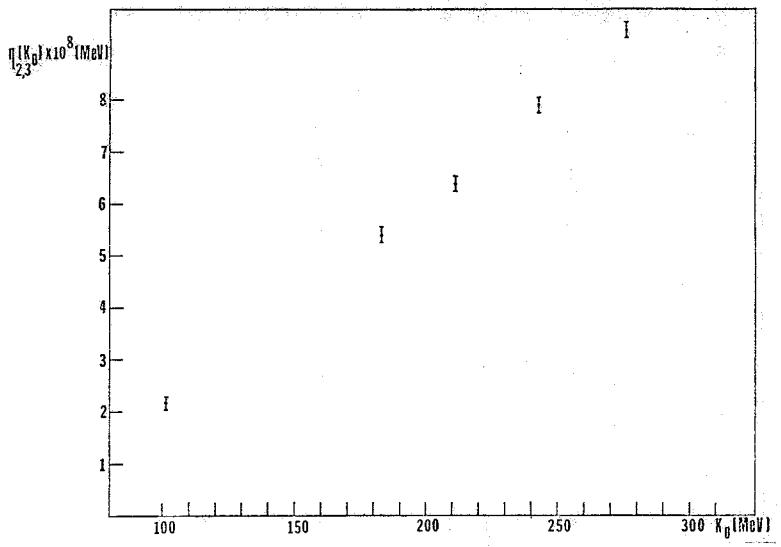

FIG. 10- Efficiency $\eta_{23}(k_o)$ for E_2P_3 couple as a function of k_o. Same parameters as Fig. 7.

7. - SPECTROMETER PERFORMANCES.

Pair spectrometer performance and comparison with theoretical calculation are reported in Figs. 11 and 12 for a primary positron beam energy E_+ = 200 MeV. In Fig. 11 counting rates per incident positron, corrected for counter detection efficiency, are given as a function of k. Fig. 12 shows the experimental spectrum $\Phi(k,B)$, obtained from the raw data of Fig. 11 by using the spectrometer efficiency values quoted in Fig. 10, compared with a Monte Carlo calculation which takes into account:

- energy spread and emittance of the positron beam;
- bremsstrahlung, annihilation, multiple scattering and energy losses of positrons in all the materials (hydrogen target, aluminium and mylar windows, air etc.) interposed in the beam path;
- photon collection line characteristics.

The integral of the evaluated intensity spectrum $\int_0^{E_+} k\Phi(k)\,dk$ agrees with the quantameter response. As results from the figure the agreement is satisfactorily within the experimental errors.

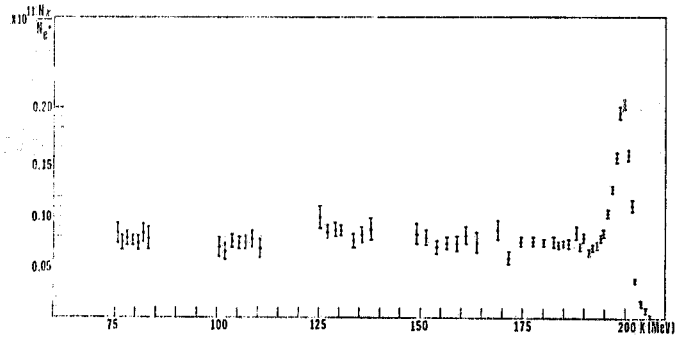

FIG. 11 - Counting rates N_γ / N_{e^+} per incident positron, corrected for counter detection efficiencies, as a function of k_o. Positron energy E_+ = 200 MeV, average positron current 12 nA, aluminium converter 5 x 10^{-3} radiation lenghts thick.

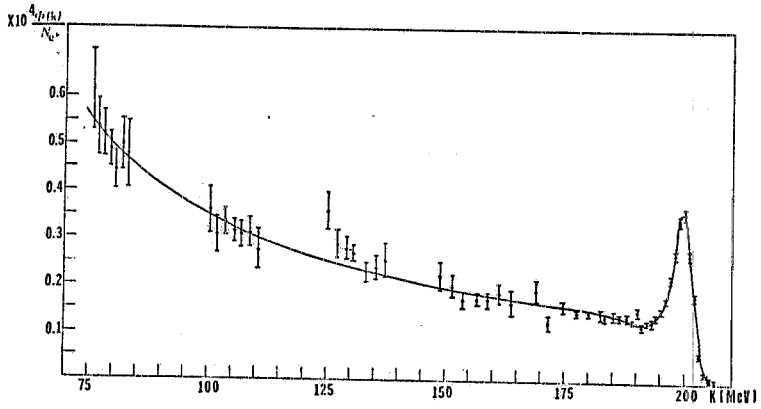

FIG. 12 - Annihilation photon spectrum $\Phi(k)/N_{e^+}$, per incident positron, obtained from data of Fig. 11 by using efficiencies $\eta_{\gamma\gamma}$. The spectrum calculated with a Monte Carlo program is also given (full line). The calculated values are normalized to the measured ones at 175 MeV; multipling factor is 1.464.

ACKNOWLEDGEMENTS

The authors would like to thank Mr. B. Dulach for the design of the spectrometer vacuum chamber. They are also indebted to the LEALE staff: M. Albicocco, A. Orlandi, W. Pesci and A. Viticchiè for their collaboration in assembling and testing the facility.

REFERENCES

(1) G.P. Capitani, E. De Sanctis, P. Di Giacomo, C. Guaraldo, G. Ricco, M. Sanzone, R. Scrimaglio and A Zucchiatti, Proc. Few Body Systems and Electromagnetic Interactions, Eds. C. Ciofi degli Atti and E. De Sanctis, Lecture Notes in Physics vol. 86 127 (Springer, 1977), and Frascati report LNF-77/45 (1977).

(2) A.P. Komar, S.P. Kruglov and I.V. Lopatin, Nucl. Instr. and Meth. 82 125 (1970).

(3) S. Pasquini and A.R. Reolon, Frascati report LNF-77/34 (1977).

(4) G.P. Capitani, E. De Sanctis, S. Pasquini and A.R. Reolon, Frascati Report LNF-78/2 (1978).

(5) Actually the focalizing properties of the magnet are poor neverthless the dispersion is good enough to enable to deal with it as a spectrometer.

(6) Two multiwire proportional chambers, 28 x 13 cm^2 sensitive area and 2 mm wire spacing, are expected to be used in a short time.

(7) V. Lucherini, Frascati report, in press.

(8) J.W. Motz, H.A. Olsen and H.W. Kock, Rev. Mod. Phys. 41, 581 (1969), eqs. 3D-1009 and 3D-1005.

(9) Y. S. Tsai, Rev. Mod. Phys. 46, 815 (1974), eqs. 3.9 and 3.38 through 3.41. In eq. 3.8 the factors Z^2 has been changed in $Z(Z+\zeta)$ where ζ is a quantity sligtly greater than unity ($\zeta \simeq 1.245$ for Al) which account for pair production in the field of electrons.

(10) The used function is a 45 terms polynominal of the type:

$$\zeta = a_1\ p+a_2 y+a_3 z^2+ a_4\ \vartheta + a_5 \cos\,(b_1 \arccos(c_1 z \cdot \varphi))+$$
$$a_6 \cos(b_2 \arccos(c_2 \Delta p^2))+ a_7 \cos(b_3 \arccos(c_3 y^2)) +$$
$$a_8 \cos(b_4 \arccos(c_4 \vartheta^2)) + a_9 \cos(b_5 \arccos(c_5\ \Delta p^2\ z^2\ \vartheta\varphi)) +$$
$$\ldots\ a_{45} \cos(b_{41} \arccos(c_{41}\ \Delta p^2\ \vartheta^2 z^2))$$

where $\Delta p = p-p_o$, with p_o momentum of the central trajectory, and a_i, b_i, c_i are convenient renormalization parameters.